Lithuanian Journal of Physics, Vol. **58**, No. 4, pp. 358–378 (2018)

NONLINEAR CORRELATIONS BETWEEN ν_1 RAMAN BAND AND GLOBAL SCALAR PROPERTIES FOR DIFFERENT LENGTH CAROTENOIDS

M. Mačernis

Institute of Chemical Physics, Faculty of Physics, Vilnius University, Saulėtekio 3, 10257 Vilnius, Lithuania
Email: mindaugas.macernis@ff.vu.lt

Received 22 March 2018; revised 15 May 2018; accepted 21 June 2018

The Raman ν_1 band corresponding to the polarization of various length carotenoid (Car) and polyene molecules was theoretically analysed using the density functional theory (DFT) approach. The polarization and other properties of Car and polyene monomers were estimated by using global scalar properties. The results demonstrate a linear dependence between the frequency of the so-called ν_1 Raman band corresponding to the C=C stretching modes, and the global hardness (and global softness) for all molecules of different conjugation lengths. Linear correlations between all global scalar properties and the conjugation length were for polyene structures only. From these calculations an additional relationship was also identified: upon *s-cis*-isomerisation the effective conjugation length and global softness increased for polyenes, while the effective conjugation length and global softness decreased for carotenoids containing β-rings at their ends. According to the electrophilicity index study, charge transfer processes (CT) should be favourable in longer carotenoid and polyene structures. A linear dependence of electronegativity was found for polyene and particular Cars subgroups. The electrophilicity index was very sensitive to special groups bonded to the polyene chain of Cars. Finally, the conjugation length of the Cars did not have a linear dependence on the electronegativity, chemical potential and electrophilicity index, but almost a linear dependence was seen on the global hardness while the polyene models had a linear dependence in all cases.

Keywords: carotenoid, polyene, resonance Raman, quantum chemistry, polarizability

PACS: 31.15.E-, 31.15.ee, 31.15.eg, 31.15.V-, 31.15.vj

1. Introduction

Carotenoids (Cars) play a number of essential functions in photosynthesis: firstly, they are involved in photoprotection of the photosynthetic apparatus [1–5]. They are responsible for efficient quenching of the excited singlet and triplet states of chlorophyll molecules [6, 7]. Cars molecules also have an important role as antioxidant agents [8–10]. Several natural carotenoids are studied as potential nanomaterial precursors for molecular photovoltaics: the larger the value of the global electronegativity and global hardness, and the smaller the global electrophilicity, the larger efficiency of the solar cell is [11].

Cars molecules display a variety of spectroscopic and functional properties, which are still poorly understood. Cars are purely linear with a conjugated polyene chain (to be more specific, it is an isoprenoid chain) and with cycle groups at the ends or with several functional groups (Fig. 1) [3]. These properties are important for absorption and Raman type spectra which vary for different length Cars in the same manner as it is for polyenes. The absorption spectrum of Cars and polyene molecules depends on the length of the conjugated chain and on the solvent properties [12–17]. The lowest electronic excited states are mainly defined by the excited states of the polyene chain: the visible spectral range corresponding to the S_0–S_2 electronic transition [18], the 'dark' S_1 state [19, 18], and other low-energy excited states [6, 20, 21]. The first excited state has the same A_g^- symmetry as the ground state and it has a double

excitation character ($HOMO^2 \rightarrow LUMO^2$) that results in the forbidden state [19, 22, 23]. The second excited state of B_u^+ symmetry is the optically allowed transition and it is mainly caused by the HOMO → LUMO transition. There is a direct relationship between the S_0–S_2 absorption band and the length of the conjugated chain [24–28] as well as with the Raman ν_1 band [29].

A vibrational technique, Raman or resonance Raman, is a direct access to the molecular properties of the electronic ground state which is very useful for Cars [30]. Resonance Raman (as well as Raman [29, 30]) spectra of Cars contain three main bands indicated as ν_1, ν_2 and ν_3 [32–34]. The ν_1 band arises from the phase stretching modes of C=C bonds; the ν_2 band arises from the C–C bond stretches coupled to the C–H in-plane bending; the ν_3 band arises from the methyl CH_3 in-plane rocking vibrations; the ν_4 band arises from the C–H out-of-plane bending modes coupled with the C=C torsion 33–35]. The ν_1 band frequency is considered as a direct access to the measure for the conjugation length of the chain [36]. For polyenes and Cars a correlation between the absorption bands and the frequencies of the ν_1 Raman band depending on their conjugation length has been experimentally identified [35]. A combination of the resonance Raman and the electronic absorption correlation is used to explain Cars absorption in different environments, including proteins and tissues [32], but even simple Car molecules in solvents should be re-examined [29, 35, 37]. Together with theoretical study the conjugation length of β-carotene is re-assessed from 11 to 9.6 double bonds [29]. This can be attributed to a partial conjugation length but its meaning for various length Cars is still under discussion [29, 31, 38]. Mainly, the partial conjugation length fits linearly to the ν_1 band of Cars or polyene Raman spectra. However, the *cis* isomerisation of the Cars ending group acts as a shorter conjugation length while it acts as a longer conjugation length for polyenes [29].

Cars are sensitive indicators of the trans-membrane electric field generated by photosynthetic charge transport [39, 40]. This is due to the large polarizability of linear conjugated chains in Cars termed as electrochromic properties [39]. The Cars background is a conjugated linear polyene chain with delocalized π-electrons with nonlinear optical properties due to ending groups [37] or introduction of electron-accepting or withdrawing substituents into their polyene backbone [41–44]. The increase in ground-state polarization induced by external field is accompanied by the increase of the degree of π-bond-order alternation within the polyene conjugated chain which can be defined as the average difference in bond orders between neighbouring carbon–carbon (CC) in the central part of the chain [44]. However, in literature there is the indirect evidence that polarizability correlates linearly according to a different conjugation length of Cars, but, as shown in calculations, the correlations were not purely linear for Cars and polyenes (Appendix, Fig. A1). The conjugation length directly represents the Raman ν_1 band for polyene and Car molecules (Fig. 2), but it is known that the Raman ν_1 band is sensitive to *s-cis* conformations at the ending groups in β-carotene [38].

In this paper the main addressed problem was understanding what is meant by a partial conjugation length, what additional information the partial conjugation length of Cars could give, and how it is correlated with global scalar properties. Using quantum chemical calculations, here we modelled the Raman spectra ν_1 and global scalar properties of nine simple carotenoids (lycopene, β-carotene (C40-β-carotene), neurosporene, lutein, spheroidene, spirilloxanthin, C50-β-carotene, C44-β-carotene, C36-β-carotene) and five different length polyene molecules (Fig. 1). The polyene molecules are model structures for Cars thus different conformations were modelled for both structures. This led us to address the influence of the extent of alternating conjugation on their Raman and global scalar properties. Analysing all global scalar properties, Cars did not have a linear dependence on the global electronegativity, chemical potential and electrophilicity index according to the Raman spectra ν_1 representing the conjugation length, differently from polyenes.

2. Quantum chemical calculations

Starting geometry for lycopene and lutein structures was taken from the protein data bank 1 LGH [45] and 1 RWT [46]. Other Cars (Fig. 1) and polyene structures [29] were artificially constructed. Calculations were performed for the Cars

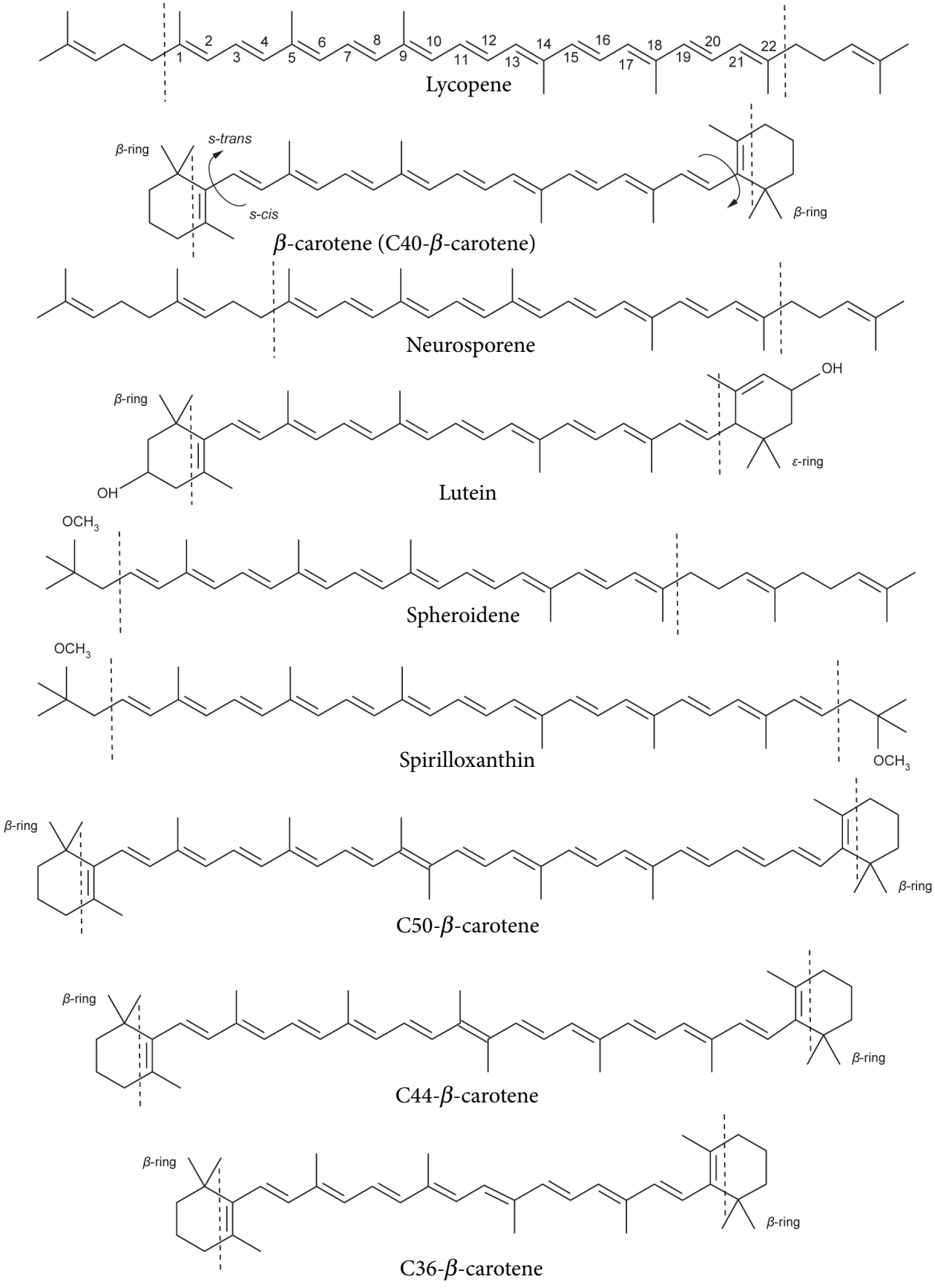

Fig. 1. Carotenoid molecular structures under consideration: lycopene, β-carotene (C40-β-carotene), neurosporene, lutein, spheroidene, spirilloxanthin, C50-β-carotene, C44-β-carotene and C36-β-carotene. Dashed lines represent the polyene chain beginnings and endings in carotenoids.

having all-*trans* conformation in their polyene chain: lycopene, neurosporene, spheroidene, lycopene, lutein, spirilloxanthin, and C50-*β*-carotene, C44-*β*-carotene, C40-*β*-carotene (*β*-carotene), C36-*β*-carotene. Calculations were performed for polyene structures with a conjugation length between 9 and 13. For these Cars the Raman analysis with experimental data has been performed previously [29]. Thus the conjugation length (*N*) was measured by numbering CC double bonds in the polyene chain as discussed in Ref. [29]. In Fig. 1 dotted lines represent the beginning and ending of the polyene chain in a specific Car molecule.

The Cars molecules differ from the pure polyene chain by their CH_3 groups conjugated with the polyene chain and their special groups (e.g. *β*-rings for *β*-carotene) at the ends of the polyene chain. The *β*-carotene type molecules (C50-*β*-carotene, C44-*β*-carotene, C40-*β*-carotene (*β*-carotene), C36-*β*-carotene) have *β*-rings at the ends of the polyene chain which are in the *s-cis*

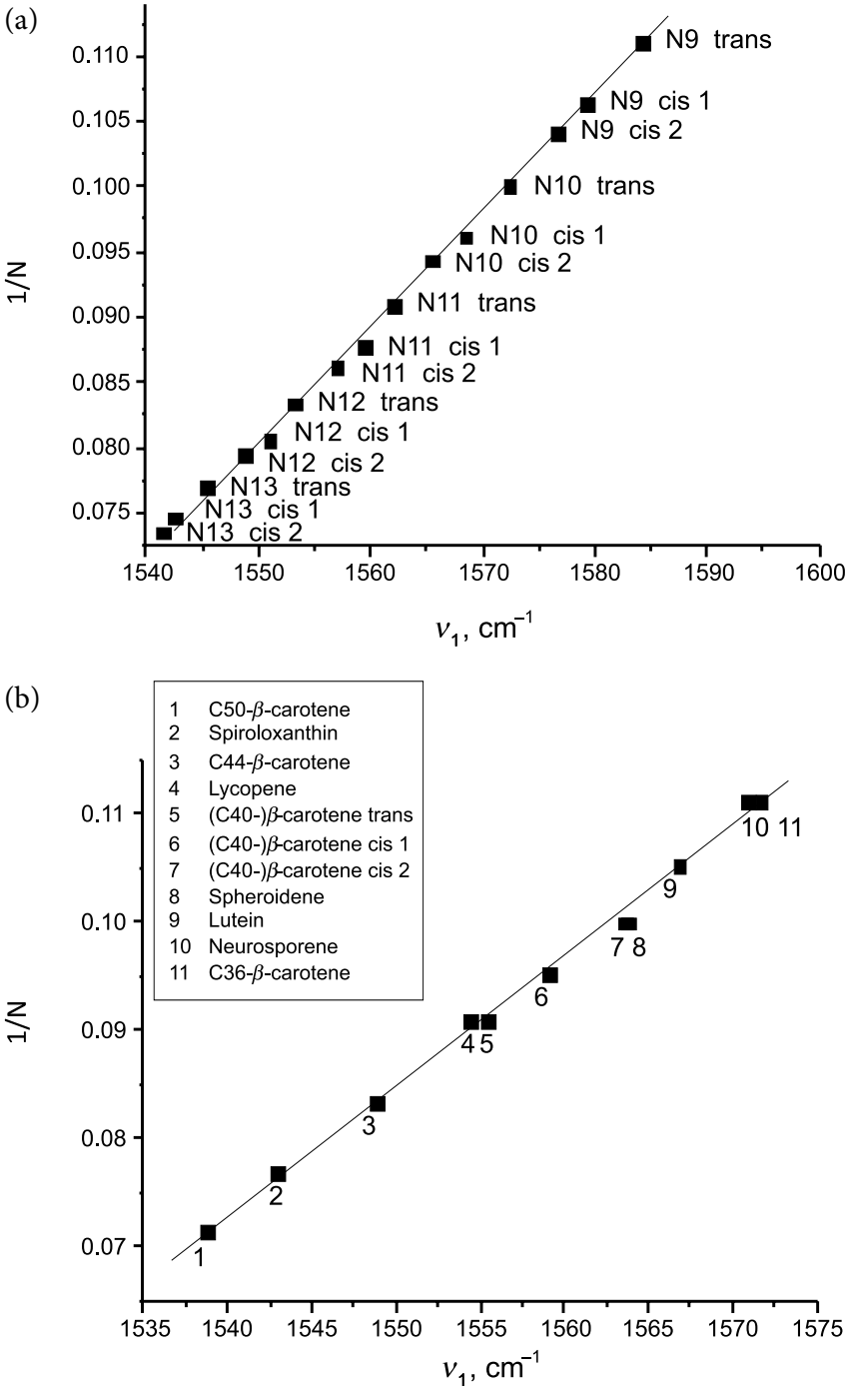

Fig. 2. Correlation between the v_1 Raman band position and the conjugated polyene chain length for different length polyenes (a) and carotenoids (b).

conformation. To analyse what happens with cyclic carotenoid molecules, computations of various polyenes and β-carotene type molecules in their both *s-cis* and *s-trans* conformations were carried out (Fig. 1). For the pure polyene chains of different lengths, containing the conjugation length from $N = 8$ to $N = 13$, calculations were performed on *all-trans*, and 1-*s-cis* and 2-*s-cis* conformations, assuming that one or both last CC units of the polyene chain are in the *s-cis* position. These typical *s-trans*, *s-cis1* and *s-cis2* transformations for polyenes and β-carotene are shown in Fig. 1 (as C40-β-carotene case).

Calculations were performed using DFT with the B3LYP functional and cc-pVDZ basis set available in the Gaussian 09 package (Rev D.01) [47]. The CAM-B3LYP is good for excitonic effects of the excited state in dimmers [48–50] but it failed for Raman intensity predictions according to experimental data as it is in previous results [29, 31]. The B3LYP functional and cc-pVDZ basis set were chosen because their results have a good agreement with the experimental data for geometries, Raman bands and excited states [29, 31, 51, 52]. The Raman spectra were analysed by attributing each Raman band to a particular vibrational mode of the molecule. Such attribution was performed in terms of quantum chemical calculations without taking into account the environmental influence on the spectrum. Thus, all calculations below were performed for Cars and polyenes in vacuum.

All carotenoid structures (Fig. 1) were optimized. Afterwards, the optimization calculations were performed for frequency and Raman. The ν_1 Raman band arises from the stretching modes of the C=C bonds [35]. All Cars structures have HOMO and LUMO orbitals on the polyene chain while the HOMO orbitals are on the double bonds [22]. For the lycopene case the HOMO and LUMO orbitals are shown in Fig. 3. Correlations between the ν_1 Raman band and global scalar properties were calculated for different length Cars. Calculations and analyses of the Wiberg bond index, natural bond orbital (NBO) partial atomic charges on C atoms and CCC angles for the polyene chain of Cars were performed. All calculations were repeated with different length polyene chains and they were compared with Cars results.

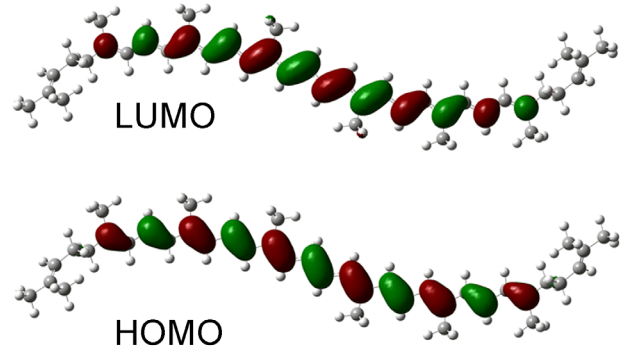

Fig. 3. The HOMO and LUMO orbitals for lycopene.

2.1. Global scalar properties

The global scalar properties such as hardness, softness, chemical potential, electronegativity and electrophilicity index are also important in determining the amount of energy required to add or remove electrons in a molecule [53]. These properties are the fundamental characteristic of chemical species, and it is used in many correlations for the estimation of thermo-physical properties [53].

The ionization potential (IP) and electron affinities (EA) are related to the HOMO and LUMO energies:

$$IP = - E_{\mathrm{HOMO}}, \tag{1}$$

$$EA = - E_{\mathrm{LUMO}}. \tag{2}$$

The difference between the HOMO and LUMO energy Δ values gives the HOMO–LUMO energy gap:

$$\Delta(E_{\mathrm{LUMO}} - E_{\mathrm{HOMO}}) = E_{\mathrm{LUMO}} - E_{\mathrm{HOMO}} = IP - EA. \tag{3}$$

By using the HOMO–LUMO energy values, five important properties can be calculated: global hardness (η), global softness (σ), electronegativity (χ), chemical potential (μ) and electrophilicity index (ω).

The global hardness η of a molecule (also it applies for an atom and an ion) is a qualitative indication of how polarizable it is, i.e. how much its electron cloud is distorted in an electric field. Molecules with a large HOMO–LUMO gap are hard which implies higher stability and opposing charge transfer, since they oppose changes in their electron density and distribution. The factor

of one half is approximate. The global hardness is a measure of molecule's ability to be polarized: the larger global hardness value the lower polarizability is:

$$\eta = \left(\frac{E_{\mathrm{LUMO}} - E_{\mathrm{HOMO}}}{2}\right) = \left(\frac{IP - EA}{2}\right). \tag{4}$$

The global softness σ is the reciprocal of the global hardness: the global softness as the inverse of global hardness. Molecules which require a small energy gap for excitation are also termed as soft molecules. They are highly polarizable in nature. In terms of chemical change, soft molecules are more reactive than hard molecules. The global softness is indicative of its ability to accept an electron. A higher softness indicates an extended molecular interaction through the hydrogen bond network or a higher π density in aromatic compounds. Thus, the larger the global softness value the higher polarizability is:

$$\sigma = \frac{1}{\eta} = \left(\frac{2}{E_{\mathrm{LUMO}} - E_{\mathrm{HOMO}}}\right) = \left(\frac{2}{IP - EA}\right). \tag{6}$$

The electronegativity χ is the tendency of molecules to attract electrons. The electronegativity of a molecule is the drop in energy when an infinitesimal amount of electronic charge is added to the system. It is the measure of resistance of an atom or an ion, or a group of atoms in a molecule for an entering electron charge. It is a useful measure of the tendency of molecules (or an atom, ion, etc.) to attract electrons:

$$\chi = -\left(\frac{E_{\mathrm{LUMO}} + E_{\mathrm{HOMO}}}{2}\right) = \left(\frac{IP + EA}{2}\right). \tag{7}$$

The chemical potential μ denotes the affinity of an electron to flee and is defined as the first derivative of the total energy with respect to the number of electrons in a molecule:

$$\mu = \left(\frac{E_{\mathrm{LUMO}} + E_{\mathrm{HOMO}}}{2}\right) = -\left(\frac{IP + EA}{2}\right). \tag{8}$$

The capability of a molecule to accept electrons is quantified as the electrophilicity index ω. The index measures the energy lowering of a substance due to the electron flow between a donor and an acceptor. In terms of the electrophilicity index it implies that it can accept more electrons:

$$\omega = \left(\frac{\mu^2}{2\eta}\right) = \left(\frac{\left(\frac{E_{\mathrm{HOMO}} + E_{\mathrm{LUMO}}}{2}\right)^2}{E_{\mathrm{LUMO}} - E_{\mathrm{HOMO}}}\right) = \left(\frac{\left(\frac{IP + EA}{2}\right)^2}{IP - EA}\right) = \left(\frac{(IP + EA)^2}{4(IP - EA)}\right). \tag{9}$$

In the case of $\Delta E = -\omega = -\left(\frac{\mu^2}{2\eta}\right)$ if $\Delta E < 0$, $\eta > 0$, the charge transfer process is energetically favourable. Thus the larger ω the more energetically favourable the charge transfer process is. Thus the electrophilicity index ω together with the hardness η are good parameters if there is the energetically favourable charge transfer (CT) process.

3. Results

3.1. Polyenes of different length

3.1.1. Geometric properties and Raman ν_1 for different length polyenes

According to the DFT calculations all polyenes had π type orbitals for the highest HOMO and the lowest LUMO orbitals. The HOMO orbitals were located on the CC double bonds while the LUMO orbital was allocated on the CC single bond as shown in Fig. 3 for a lycopene molecule.

The polyenes had a linear correlation between the conjugation length N and the Raman ν_1 band (Fig. 2(a)). The largest ν_1 value (1584.15 cm^{-1}) was for the shortest all-*trans*-polyene with $N = 9$. The lowest ν_1 value (1545.32 cm^{-1}) was for the longest all-*trans*-polyene with $N = 13$. The *cis* transformation of the last CC double bond was lowering the Raman ν_1 band which could quite easily be fitted on the same line (Fig. 2(a)). The $1/N$ fitted value for the *s-cis1* type transformation was 42.6–41.8% in the position between two N and $N + 1$ length *s-trans* type structures. The $1/N$ fitted value for the *s-cis2* type transformation was 62.5–61.8% in the position between two N and $N + 1$ length *s-trans* type structures.

The Wiber bond index values were calculated for the polyenes with the length N between 9 and 13 which had *s-trans*, *s-cis1* and *s-cis2* geometrical conformations. The average CC double bond

Wiber bond index was lower for the longer polyene chain (Appendix, Table 1A): it was 1.68 for $N = 9$ and 1.66 for $N = 13$. In the case of $N = 9$ polyene, after the *s-cis2* transformation the average Wiber bond index value increased up to 1.69. The sum of Wiber bond index values was not in a linear correlation when they were summed over the all CC double bond. In all cases the Wiber bond index had small differences between the same N length polyene in *s-trans*, *s-cis1* and *s-cis2* geometrical conformations. The central CC double and CC single bonds had almost the same values for all length polyene chains (Appendix, 1A).

NBO atomic charges on C atoms in the polyene chain were calculated (Appendix, Table 2A) for the polyenes with the length N between 9 and 13 which had *s-trans*, *s-cis1* and *s-cis2* geometrical conformations. The average NBO atomic charge on C atoms was less negative for the longer polyene chain (Appendix, Table 2A): it was –0.229 for $N = 13$ and –0.236 for $N = 9$. In the case of $N = 12$ polyene after the *s-cis2* transformation, the average NBO atomic charges on the C value decreased by 0.001. The sum of NBO charges on C atoms were not in a linear correlation when they were summed over the C atoms. In all cases the NBO atomic charges on C atoms had small differences between the same N length polyene in *s-trans*, *s-cis1* and *s-cis2* geometrical conformations. The central C atoms had the same –0.214 value for all length polyene chains (Appendix, Table 2A).

Other geometrical properties of the polyenes were analysed such as the length of CC bonds, dihedral angles between CCCC and angles between CCC. There was a major difference in the CCC angles only. Thus they were listed out to look for some additional possible correlations (Supp. Inf. Table 3A). The average CCC angle was larger for the longer polyene chain: it was 124.90 for $N = 13$ and 124.44 for $N = 9$. In the *s-cis1* and *s-cis2* conformations the CCC angle changed to the dihedral angle. These changes involved the average CCC angle larger than the polyene length increment: the difference of the average CCC angle between *N*9 *s-trans* and *N*9 *s-cis2* was 0.66 while the difference between *N*9 *s-trans* and *N*13 *s-trans* was 0.01. Similar results were with the CCC angle sums of all values.

3.1.2 Global scalar properties and Raman ν_1 for polyenes

In Fig. 4, the correlations of global scalar properties with Raman ν_1 for different length polyenes are shown. There was a linear dependence for all four global scalar properties: global hardness (A), electronegativity (B), chemical potential (C) and electrophilicity index (D). The HOMO and LUMO orbital energies were lower for the shorter length N all-*trans* polyenes. The HOMO orbital energies were from –0.1788 a.u. for the polyene of $N = 9$ to –0.1714 a.u. for the polyene of $N = 13$. The LUMO orbital energies were from –0.0546 a.u. for the polyene $N = 9$ to –0.074 a.u. for the polyene $N = 13$. Thus the HOMO and LUMO energy gaps Δ were smaller for the longer polyene and they depended linearly.

The largest global hardness $\eta = 1.69$eV was for the $N = 9$ all-*trans*-polyene (Fig. 4(a)). It was 1.66 and 1.63 eV for the *s-cis1* and *s-cis2* conformations, respectively. There was a similar trend for the longer polyene structures. The smallest global hardness $\eta = 1.3$ eV was for the $N = 13$ *s-cis2* conformation polyene. The linear dependence was similar as it was with the conjugation length (Fig. 2(b)).

The largest electronegativity $\chi = 3.36$ eV was for the $N = 13$ *s-cis2* conformation polyene (Fig. 4(b)). It was 3.35 and 3.34 eV for the *s-cis1* and *s-trans* conformations, respectively. There was a similar trend for the longer polyene structures. The smallest electronegativity $\chi = 3.18$ eV was for the $N = 9$ *s-trans* conformation polyene.

The largest chemical potential $\mu = -3.18$ eV was for the $N = 9$ all-*trans*-polyene (Fig. 4(c)). It was –3.2 and –3.22 eV for the *s-cis1* and *s-cis2* conformations, respectively. There was a similar trend for the longer polyene structures. The smallest chemical potential $\mu = -3.36$ eV was for the $N = 13$ *s-cis2* conformation polyene. The linear dependence was similar as it was with the conjugation length (Fig. 2(b)).

The largest electrophilicity index $\omega = 4.35$ was for the $N = 13$ *s-cis2* conformation polyene (Fig. 4(d)). It was 4.29 and 4.21 for the *s-cis1* and *s-trans* conformations, respectively. There was a similar trend for the longer polyene structures. The smallest electrophilicity index $\omega = 2.99$ was for the $N = 9$ *s-trans* conformation polyene.

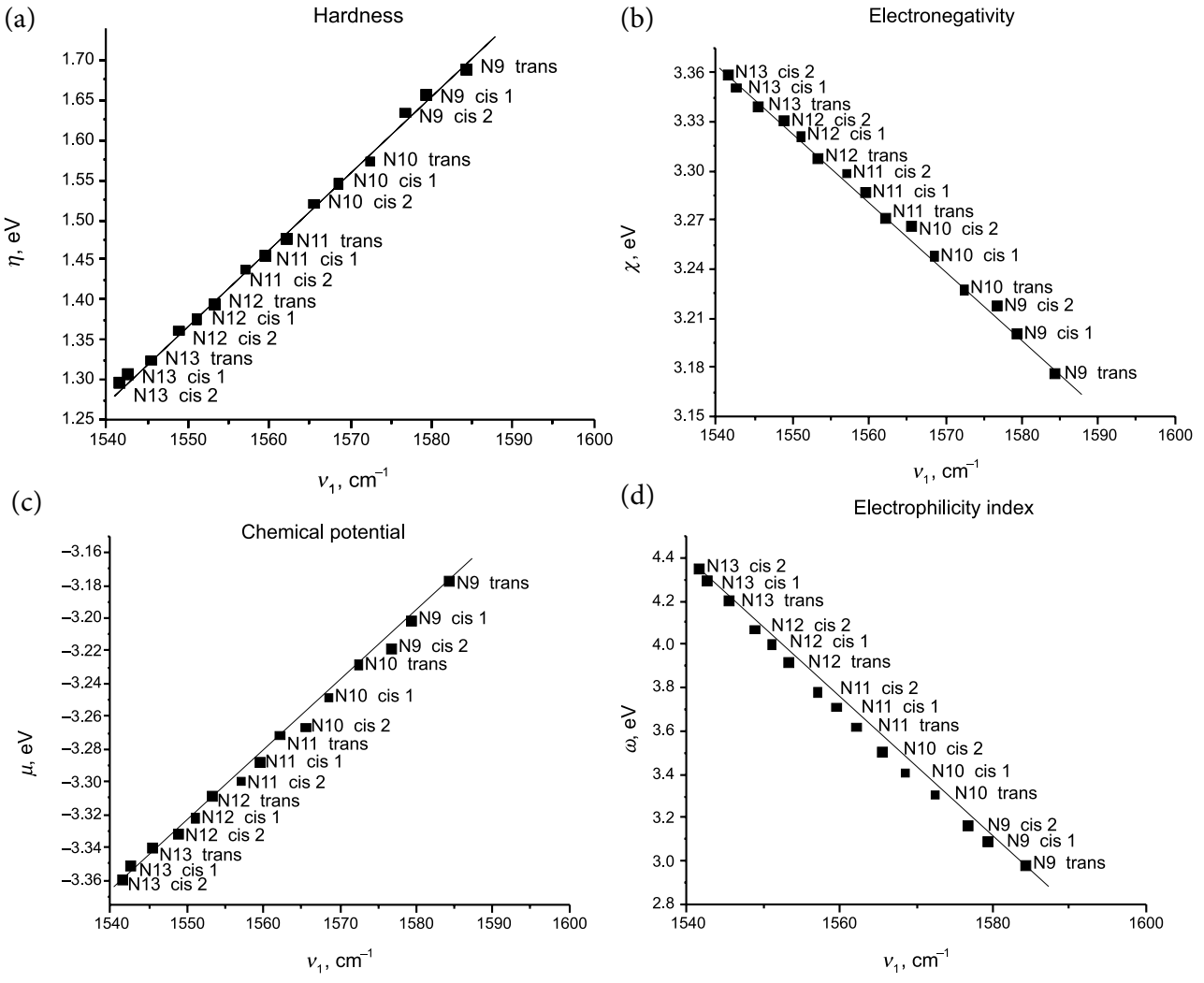

Fig. 4. A linear correlation between the ν_1 Raman band position and global hardness (a), electronegativity (b), chemical potential (c), electrophilicity index (d) for different length polyenes.

3.2. Carotenoids of different length

3.2.1. Geometric properties and Raman ν_1 for different length carotenoids

The analysed Cars were of two types (Fig. 1): the first group molecules were lycopene, neurosporene, spheroidene and spirilloxanthin; the second group molecules were lutein and *β*-Cars: *β*-carotene (C40-*β*-carotene), C50-*β*-carotene, C44-*β*-carotene and C36-*β*-carotene. The first group fitted linearly according to the conjugation length $1/N$ and the Raman ν_1 band (Fig. 2(b)). The second *β*-Cars group had a linear dependence according to the conjugation length $1/N$ and the Raman ν_1 band (Fig. 2(b)) if the N values were fitted on one line. This fact resulted in the partial conjugation length. The N values were 14, 12, 10, 9.5 and 9 for C50-*β*-carotene, C44-*β*-carotene, C40-*β*-carotene, lutein and C36-*β*-carotene, respectively. C40-*β*-carotene was considered as a model for the analyses of *s-trans*, *s-cis1* and *s-cis2* conformations. The *s-cis2* conformation represents a C40-*β*-carotene structure. The N values 11, 10.5 and 10 were for the *s-trans*, *s-cis1* and *s-cis2* of C40-*β*-carotene structures. The fitted values had a different tendency after *s-trans* and *s-cis* transformations than it was for pure polyene chains (Fig. 2(a)).

According to the DFT calculations, all Cars had *π* type orbitals for the three highest HOMO and the three lowest LUMO orbitals. The HOMO orbital was located on the CC double bonds while the LUMO orbital was located on the CC single bond for all Cars, as shown in Fig. 3 for a lycopene molecule.

The Wiber bond index values were calculated for all investigated Cars. The average CC double bond Wiber bond index was lower for the Cars having a longer polyene chain (Appendix, Table 1B): it was 1.63 for C50-β-carotene and 1.66 for C36-β-carotene. In the case of lutein, it was 1.65 what was between those of C36-β-carotene (1.66) and neurosporene (1.64). This result did not correlate with the fitted conjugation length (Fig. 2(b)) where the lutein average Wiber bond index would be expected to be the lowest one. Also the sum of Wiber bond index values was not in a linear correlation when they were summed over the all CC double bond. In all cases the Wiber bond index had quite large differences between the same C40-β-carotene *s-trans*, *s-cis1* and *s-cis2* conformations: 1.63, 1.64 and 1.65. The central CC double bonds had almost the same values, about 1.6, for all Cars (Appendix, Table 1B).

NBO atomic charges on C atoms in the polyene chain were calculated (Appendix, Table 2B) for all Cars. The average NBO atomic charge on C atoms was less negative for the Cars having a longer polyene chain (Appendix, Table 1B): it was –0.153 for C50-β-carotene and –0.14 for C36-β-carotene. In the case of lutein it was –0.158 what was between those of C36-β-carotene (–0.14) and neurosporene (–0.162). This result did not correlate with the fitted conjugation length (Fig. 2A) where the lutein average NBO atomic charge on C atoms would be expected to be the largest one. In all cases, the average NBO atomic charge on C atoms was quite similar between the same C40-β-carotene *s-trans*, *s-cis1* and *s-cis2* conformations: –0.146, 1–0.147 and –0.147. Also the sum of NBO atomic charge values was not in a linear correlation when they were summed over all C atoms in the polyene chain. The central C atoms had values from –0.217 to –0.024 for different Cars (Appendix, Table 1B).

Other geometrical properties of the Cars were analysed: the length of CC bonds, dihedral angles between CCCC and angles between CCC. As with the polyene structures, there was a major difference in the CCC angles. Thus they were listed out to look for some additional possible correlations (Appendix, Table 3B). The average CCC angle varies for different Cars: it is 124.09, 124.41 and 124.1 for C50-β-carotene, lycopene and lutein, respectively. As expected in the C40-β-carotene *s-cis1* and *s-cis2* conformations, the CCC angle changed to the dihedral angle and β-ring interactions. These changes involved the average CCC angle larger than the polyene length increment: the difference of the average CCC angle between C40-β-carotene *s-trans* and C40-β-carotene *s-cis2* was 0.17 while the difference between C50-β-carotene and lutein was 0.01. Similar results were with the CCC angle sums of all values.

3.2.2. Global scalar properties and Raman ν_1 for Cars

Figure 5 shows the correlations of global scalar properties with Raman ν_1 for different Cars: global hardness (A), electronegativity (B), chemical potential (C) and electrophilicity index (D). The HOMO and LUMO orbital energies varied between different length Cars. The lowest HOMO orbital energy (–0.1722 eV) was for lutein and the highest HOMO orbital energy (–0.1627 eV) was for spirilloxanthin. The lowest LUMO orbital energy (–0.0674 eV) was for C50-β-carotene and the highest LUMO orbital energy (–0.0433 eV) was for spirilloxanthin. The HOMO and LUMO energy gaps Δ for Cars depended non-linearly but they were smaller for the Cars having longer polyene chains.

For Cars there was a linear dependence between the Raman ν_1 and the global hardness η. The largest global hardness η = 1.7 eV was for C36-β-carotene (Fig. 5(a)). The smallest global hardness η = 1.31 eV was for C50-β-carotene. The C40-β-carotene *s-trans*, *s-cis1* and *s-cis2* conformations had 1.503, 1.547 and 1.602 η, respectively. The conformation had a different tendency than it was with all polyene structures (Fig. 4(a)). The linear dependence for all Cars was similar as it was with the conjugation length (Fig. 2(b)).

The electronegativity χ values had a linear dependence with the Raman ν_1 only within the same type Cars structures (Fig. 5(b)). There was a linear dependence between C50-β-carotene, C44-β-carotene, C40-β-carotene (*s-cis2*) and C36-β-carotene which had χ values 3.14, 3.06, 2.96 and 2.9 eV, respectively. The other values vary for different Cars (Fig. 5(b)): the largest electronegativity χ = 3.07 eV was for spirilloxanthin, the smallest electronegativity χ = 2.86 eV was for neurosporene.

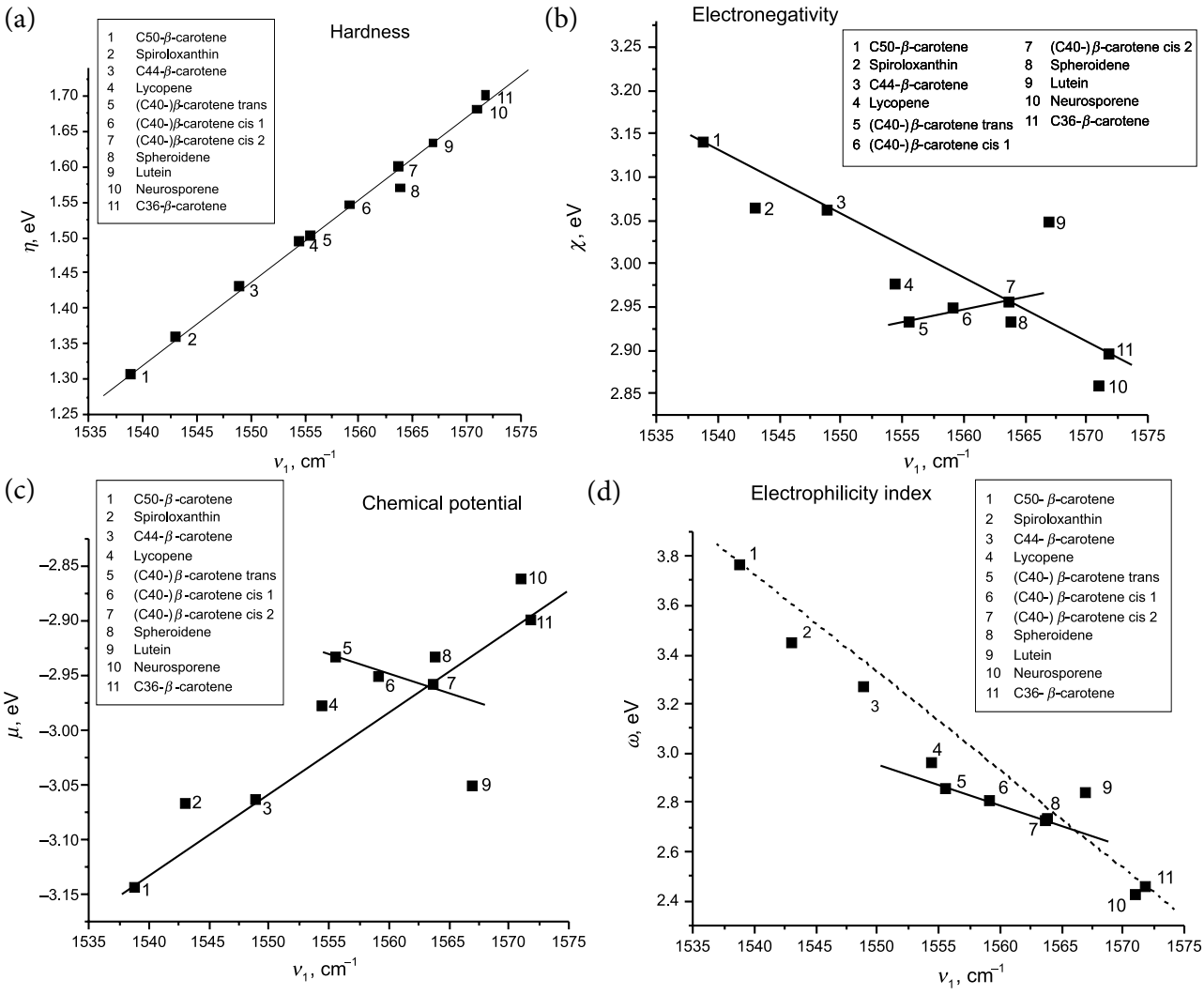

Fig. 5. The linear and nonlinear correlation between the ν_1 Raman band position and global hardness (a), electronegativity (b), chemical potential (c), electrophilicity index (d) for different length carotenoids and their subgroups.

The chemical potential μ values also had a linear dependence with Raman ν_1 only within the same type Cars structures (Fig. 5(c)). There was a linear dependence between C50-β-carotene, C44-β-carotene, C40-β-carotene (*s-cis2*) and C36-β-carotene which had μ values –3.14, –3.06, –2.96 and –2.9 eV, respectively. The other values vary for different Cars (Fig. 5(c)): the largest chemical potential μ = –2.86 eV was for neurosporene, the smallest chemical potential μ = –3.05 eV was for lutein.

For Cars the electrophilicity index ω had an unclear correlation with the Raman ν_1 band (Fig. 5(d)). The largest electrophilicity index ω = 3.77 was for C50-β-carotene, the smallest electrophilicity index ω = 2.43 was for neurosporene.

So for Cars there was a linear dependence between the Raman ν_1 and the global hardness η (Fig. 6(a)) which was similar as it was with the conjugation length (Fig. 2(b)). Figure 6(a) shows the dependence between the conjugation length $1/N$ and the global hardness η. Figure 6(b) shows the dependence between the conjugation length N and the global softness σ because of the relation in Eq. (6).

4. Discussion

The polarizability can also be measured by global hardness and global softness values. According to the calculations, the polarizability became larger for longer polyenes and Cars, but the trends were different. Moreover, the direct polarizability, e.g. isotropic and anisotropic polarizabilities (see Appendix, Eqs. (A1), (A2)) of Cars and polyenes, does not have a pure linear correlation (Appendix, Fig. A1). The higher values of global softness

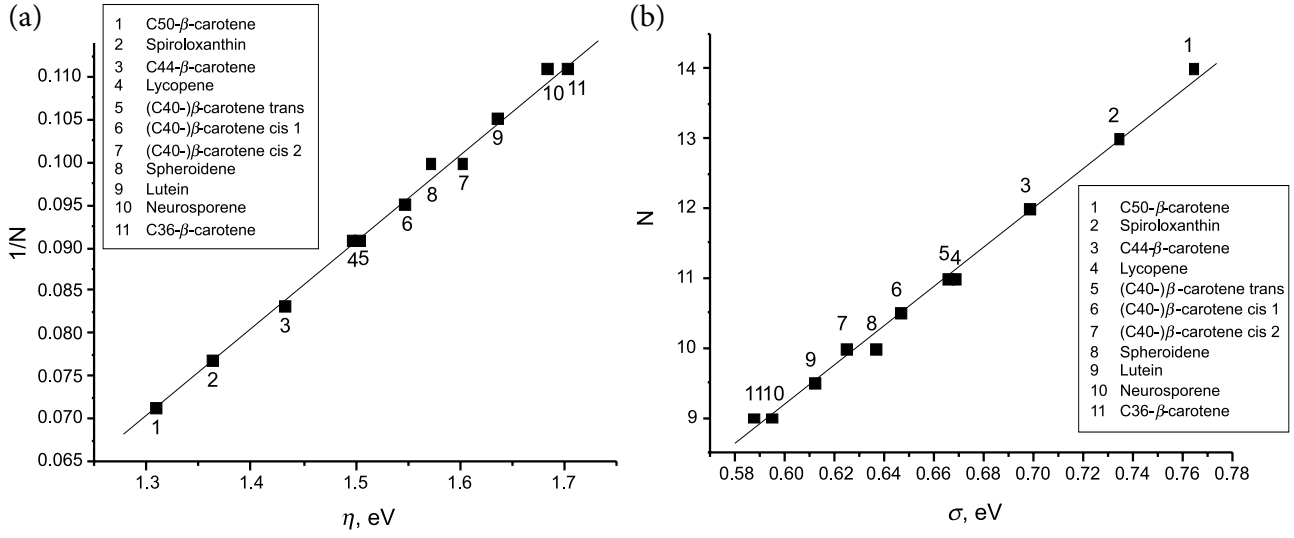

Fig. 6. The correlation between the conjugated polyene chain length and the global hardness (a), global softness (b) for different length carotenoids.

indicate an extended molecular interaction through the hydrogen bond network or a higher π density which may be important in longer Cars for excited state dynamics [38]. For the polyenes the global hardness and global softness values depended on the linear tendency: the longer polyene the larger polarizability (Fig. 4(a)). The same trend was clearly seen for the Cars (Fig. 5(a)). The *s-cis* conformation in polyenes increased the polarizability due to the extent of alternating conjugation in the structure. However, β-carotene in the *s-cis* conformation resulted in lower values which is due to the fact that the π orbital inside the β-ring is separated from the polyene chain (π density decreases).

Electronegativity χ is a useful measure of the tendency of Cars and polyenes to attract electrons. It depends linearly according to the polyene length. This was not true for Cars as one group while it was true for subgroups: β-Cars or between β-carotene structures having *s-cis2* conformations (Fig. 5(b)). However, this means that the increased electronegativity in longer polyene chains of the same group molecules (polyene, β-Cars) is favourable to attract electron densities towards itself but could vary from Car to Car (Figs. 4(b) and 5(b)).

The electrophilicity index ω implies that a molecule can accept more electrons what means that longer polyenes can accept more electrons than shorter polyenes (Fig. 4(d)). The tendency was linear for the polyene structures but not for all Cars or subgroup β-Cars (Fig. 5(d)), still there were linear correlations between the β-carotene *cis* type conformers. However, the Cars with a longer polyene chain had a larger electrophilicity index trend as it was with the polyene structures. This non-linear dependence can be attributed to distortions effected additional groups in the middle of the polyene chain of Cars (Fig. 1).

The longer N polyene structures and Cars having the longer polyene chains had larger ω (Figs. 4(d) and 5(d)). Thus it means that the CT process should be favourable in longer Cars.

For the larger efficiency of the solar cell with the Cars it is important that the larger the value of the global electronegativity and global hardness, the smaller the global electrophilicity is [11]. The electrophilicity index ω showed that it was sensitive to additional groups in the middle of the polyene chain according to the calculations for Cars and polyene. Thus such additional groups can be (e.g. Ref. [31]) in Cars what means that the specific electrophilicity index may be chosen. The electronegativity χ was sensitive to the ending groups of Cars which can be concluded from the fact that there is a linear dependence for the Cars subgroups (β-Cars, ending group *cis* isomerization).

5. Conclusions

This study provides the theoretical framework to explain global scalar properties, polarizability effects and changes in the effective conjugation

length of Cars molecules which can easily be distinguished due to a different correlation between the frequency of the ν_1 Raman band and their global scalar properties. The analyses of NBO and Wiberg bond indices are not useful for different length conjugation trends because results vary for different length Cars as well as for different length polyenes. There was a linear correlation between the global hardness and the conjugation length N of polyene and Cars: the longer the chain, the higher the global softness parameter. The Raman ν_1 band shift cannot be attributed to the increased polarizability in the Cars environments while some correlations exist. Vibrational frequencies are dictated by the potential energy surface but there were not systematic changes between different length conjugation chains by analysing NBO or Wiberg bond indices. Also according to the electrophilicity index study charge transfer (CT) processes were favourable in longer Cars structures. The CT process may be controlled by internal molecular structures of such CH_3 groups or endings of Cars (e.g. β-rings). All global scalar properties depended linearly for polyenes but this was not true for Cars. Electronegativity linearly depended for Cars subgroups: β-Cars or ending group *cis* isomerization. The electrophilicity index was very sensitive to special groups bonded to the polyene chain of Cars. Also there was not a pure linear correlation between the conjugation length and the Raman ν_1 band for Cars and for polyenes. Finally, the conjugation length of the Cars did not have a linear dependence on the electronegativity, chemical potential and electrophilicity index, but almost a linear dependence was seen on the global hardness while the polyene models had a linear dependence in all cases.

Acknowledgements

The public access supercomputer from the High Performance Computing Center (HPCC) of the Lithuanian National Center of Physical and Technology Sciences (NCPTS) at the Faculty of Physics of Vilnius University was used. M. M. acknowledges the COST Project EUROCAROTEN (CA COST Action CA15136). This work is funded by the Research Council of Lithuania (LMT Grant No. MIP080/2015).

Appendix

The polarizability has six unique components: α_{xx}, α_{xy}, α_{yy}, α_{xz}, α_{yz}, α_{zz}. The isotropic and anisotropic polarizability can be expressed as

$$\alpha_{\text{iso}} = \frac{1}{3}(\alpha_{xx} + \alpha_{yy} + \alpha_{zz}), \tag{A1}$$

$$\alpha_{\text{aniso}} = \frac{1}{\sqrt{2}} \times \tag{A2}$$

$$\times\sqrt{(\alpha_{xx}-\alpha_{yy})^2+(\alpha_{xx}-\alpha_{zz})^2+(\alpha_{yy}-\alpha_{zz})^2+6(\alpha_{xy}^2+\alpha_{xz}^2+\alpha_{yz}^2)}.$$

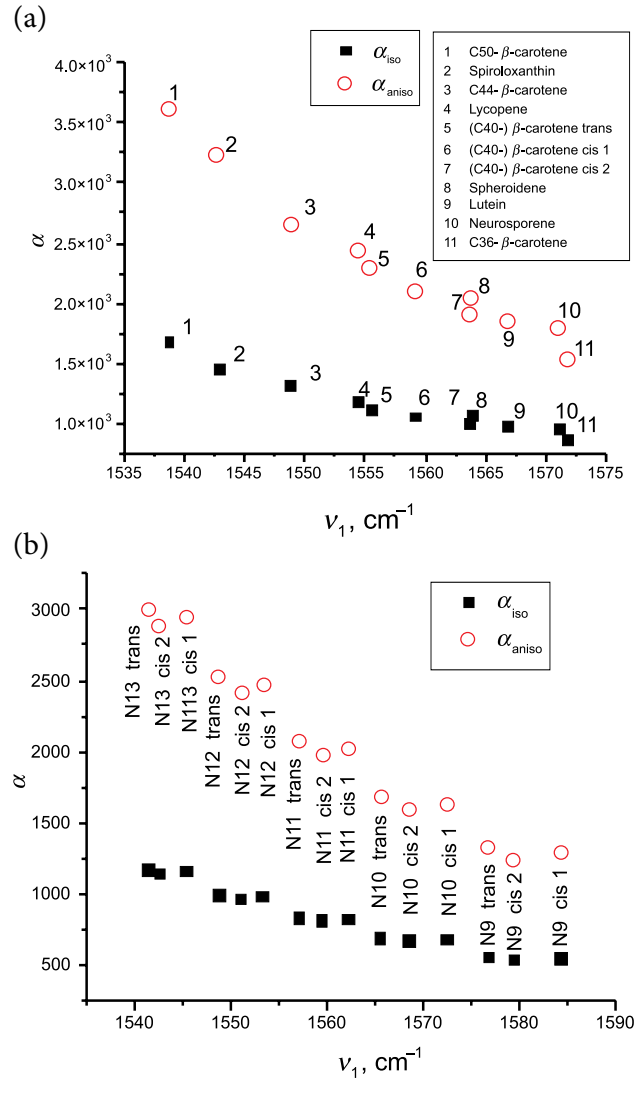

Fig. A1. Isotropic and anisotropic polarizability values according to the Raman ν_1 band for different length Cars (a) and polyene (b). There is a similar picture according to the partial conjugation length because of a linear correlation between the Raman ν_1 band and the conjugation length.

Table 1. C–C bond Wiberg bond index in the polyene chain for the calculated optimized geometries. Central bonds are coloured with a grey background. The *s-trans* and *s-cis* represent the positions of the ending groups. A: values for different length polyene molecules. B: values for carotenoids.

A

Bond	$N = 9$			$N = 10$			$N = 11$			$N = 12$			$N = 13$		
	s-trans	*s-cis1*	*s-cis2*	*s-trans*	*s-cis*1	*s-cis2*	*s-trans*	*s-cis1*	*s-cis2*	*s-trans*	*s-cis1*	*s-cis2*	*s-trans*	*s-cis1*	*s-cis2*
1–2	1.84	1.84	1.86	1.84	1.84	1.85	1.84	1.84	1.86	1.84	1.84	1.86	1.84	1.84	1.86
2–3	1.17	1.17	1.14	1.17	1.17	1.15	1.17	1.17	1.15	1.17	1.17	1.15	1.17	1.17	1.15
3–4	1.67	1.67	1.68	1.67	1.67	1.68	1.67	1.67	1.68	1.67	1.67	1.68	1.67	1.67	1.68
4–5	1.21	1.21	1.21	1.21	1.21	1.21	1.21	1.21	1.21	1.21	1.21	1.21	1.21	1.21	1.21
5–6	1.64	1.64	1.63	1.63	1.63	1.63	1.63	1.63	1.63	1.63	1.63	1.63	1.63	1.63	1.63
6–7	1.22	1.22	1.22	1.22	1.22	1.23	1.22	1.22	1.23	1.23	1.23	1.23	1.23	1.23	1.23
7–8	1.62	1.62	1.62	1.62	1.62	1.61	1.62	1.62	1.61	1.62	1.62	1.61	1.61	1.61	1.61
8–9	1.23	1.23	1.23	1.23	1.23	1.23	1.23	1.23	1.23	1.23	1.23	1.24	1.23	1.24	1.24
9–10	1.62	1.62	1.61	1.61	1.61	1.61	1.61	1.61	1.61	1.61	1.61	1.60	1.61	1.60	1.60
10–11	1.23	1.23	1.23	1.23	1.23	1.23	1.24	1.24	1.24	1.24	1.24	1.24	1.24	1.24	1.24
11–12	1.62	1.62	1.62	1.61	1.61	1.61	1.61	1.61	1.60	1.60	1.60	1.60	1.60	1.60	1.60
12–13	1.22	1.22	1.22	1.23	1.23	1.23	1.24	1.24	1.24	1.24	1.24	1.24	1.24	1.24	1.24
13–14	1.64	1.63	1.63	1.62	1.62	1.61	1.61	1.61	1.61	1.60	1.60	1.60	1.60	1.60	1.60
14–15	1.21	1.21	1.21	1.22	1.23	1.23	1.23	1.23	1.23	1.24	1.24	1.24	1.24	1.24	1.24
15–16	1.67	1.68	1.68	1.63	1.63	1.63	1.62	1.61	1.61	1.61	1.61	1.60	1.60	1.60	1.60
16–17	1.17	1.15	1.14	1.21	1.21	1.21	1.22	1.23	1.23	1.23	1.23	1.24	1.24	1.24	1.24
17–18	1.84	1.86	1.86	1.67	1.68	1.68	1.63	1.63	1.63	1.62	1.61	1.61	1.61	1.60	1.60
18–19				1.17	1.15	1.15	1.21	1.21	1.21	1.23	1.23	1.23	1.23	1.24	1.24
19–20				1.84	1.85	1.85	1.67	1.68	1.68	1.63	1.63	1.63	1.61	1.61	1.61
20–21							1.17	1.15	1.15	1.21	1.21	1.21	1.23	1.23	1.23
21–22							1.84	1.85	1.86	1.67	1.68	1.68	1.63	1.63	1.63
22–23										1.17	1.15	1.15	1.21	1.22	1.21
23–24										1.84	1.85	1.86	1.67	1.68	1.68
24–25													1.17	1.15	1.15
25–26													1.84	1.85	1.86
AVG*	1.68	1.68	1.69	1.68	1.68	1.68	1.67	1.67	1.67	1.66	1.66	1.66	1.66	1.66	1.66
SUM*	15.16	15.16	15.18	16.75	16.76	16.76	18.34	18.35	18.37	19.94	19.94	19.96	21.53	21.52	21.54

* C=C type bonds.

B

Bond	C50-β-carotene	Spiroloxanthin	C44-β-carotene	Lycopene	(C40-)β-carotene			Spheroidene	Lutein	C36-β-carotene	Neurosporene
					s-trans	*s-cis1*	*s-cis2*				
1–2	1.74	1.79	1.74	1.73	1.70	1.70	1.75	1.79	1.79	1.75	1.73
2–3	1.08	1.14	1.08	1.17	1.14	1.14	1.08	1.14	1.14	1.08	1.17
3–4	1.73	1.63	1.73	1.67	1.68	1.68	1.73	1.63	1.63	1.73	1.67
4–5	1.16	1.20	1.16	1.18	1.17	1.17	1.15	1.20	1.20	1.16	1.18
5–6	1.61	1.64	1.61	1.59	1.60	1.60	1.61	1.64	1.64	1.61	1.59
6–7	1.21	1.19	1.21	1.22	1.22	1.22	1.21	1.19	1.19	1.21	1.23
7–8	1.63	1.58	1.63	1.62	1.62	1.62	1.63	1.58	1.57	1.63	1.61
8–9	1.19	1.23	1.19	1.20	1.20	1.20	1.19	1.22	1.23	1.19	1.23
9–10	1.58	1.61	1.58	1.57	1.57	1.57	1.57	1.62	1.61	1.57	1.57
10–11	1.23	1.20	1.23	1.24	1.24	1.24	1.24	1.20	1.23	1.23	1.20
11–12	1.61	1.56	1.61	1.60	1.60	1.60	1.60	1.57	1.57	1.57	1.62
12–13	1.21	1.24	1.20	1.24	1.24	1.24	1.24	1.23	1.19	1.19	1.22
13–14	1.56	1.59	1.53	1.57	1.57	1.57	1.57	1.61	1.63	1.63	1.60
14–15	1.24	1.24	1.20	1.20	1.20	1.20	1.19	1.23	1.21	1.21	1.18
15–16	1.59	1.56	1.61	1.62	1.62	1.63	1.63	1.59	1.61	1.61	1.67
16–17	1.24	1.20	1.23	1.22	1.22	1.21	1.21	1.18	1.16	1.16	1.17
17–18	1.56	1.61	1.58	1.59	1.60	1.61	1.61	1.67	1.73	1.73	1.73
18–19	1.21	1.23	1.19	1.18	1.17	1.16	1.16	1.17	1.08	1.08	
19–20	1.61	1.58	1.63	1.67	1.68	1.73	1.73	1.73	1.75	1.75	
20–21	1.23	1.19	1.21	1.17	1.14	1.08	1.08				
21–22	1.58	1.64	1.61	1.73	1.70	1.74	1.75				
22–23	1.19	1.20	1.15								
23–24	1.63	1.63	1.73								
24–25	1.21	1.14	1.08								
25–26	1.61	1.79	1.75								
26–17	1.16										
27–28	1.73										
28–29	1.08										
29–30	1.74										
AVG*	1.63	1.63	1.64	1.63	1.63	1.64	1.65	1.64	1.65	1.66	1.64
SUM*	24.49	21.20	21.33	17.95	17.91	18.04	18.18	16.41	16.51	16.58	14.78

* C=C type bonds.

Table 2. NBO atomic charges on C atoms in the polyene chain for the calculated optimized geometries. Central bonds are coloured with a grey background. The *s-trans* and *s-cis* represent the positions of the ending groups. A: values for different length polyene molecules. B: values for carotenoids.

A

Atom	$N = 9$			$N = 10$			$N = 11$			$N = 12$			$N = 13$		
	s-trans	*s-cis1*	*s-cis2*	*s-trans*	*s-cis1*	*s-cis2*	*s-trans*	*s-cis1*	*s-cis2*	*s-trans*	*s-cis1*	*s-cis2*	*s-trans*	*s-cis1*	*s-cis2*
1	−0.387	−0.387	−0.383	−0.387	−0.387	−0.382	−0.387	−0.387	−0.382	−0.387	−0.387	−0.382	−0.387	−0.387	−0.382
2	−0.240	−0.240	−0.247	−0.240	−0.240	−0.247	−0.240	−0.240	−0.247	−0.240	−0.240	−0.247	−0.240	−0.240	−0.247
3	−0.212	−0.212	−0.221	−0.212	−0.212	−0.221	−0.212	−0.212	−0.221	−0.212	−0.212	−0.221	−0.212	−0.212	−0.221
4	−0.217	−0.217	−0.208	−0.218	−0.218	−0.207	−0.218	−0.218	−0.208	−0.218	−0.218	−0.208	−0.218	−0.218	−0.208
5	−0.212	−0.212	−0.210	−0.212	−0.212	−0.210	−0.212	−0.212	−0.210	−0.212	−0.212	−0.210	−0.212	−0.211	−0.210
6	−0.215	−0.215	−0.216	−0.215	−0.215	−0.216	−0.215	−0.215	−0.216	−0.215	−0.215	−0.216	−0.215	−0.215	−0.216
7	−0.213	−0.213	−0.213	−0.213	−0.213	−0.213	−0.213	−0.213	−0.213	−0.213	−0.213	−0.213	−0.213	−0.213	−0.213
8	−0.214	−0.214	−0.214	−0.214	−0.214	−0.214	−0.214	−0.214	−0.214	−0.214	−0.214	−0.214	−0.215	−0.215	−0.214
9	−0.214	−0.214	−0.214	−0.214	−0.213	−0.213	−0.213	−0.213	−0.213	−0.213	−0.213	−0.213	−0.213	−0.213	−0.213
10	−0.214	−0.214	−0.214	−0.214	−0.214	−0.214	−0.214	−0.214	−0.214	−0.214	−0.214	−0.214	−0.214	−0.214	−0.214
11	−0.214	−0.214	−0.214	−0.214	−0.214	−0.214	−0.214	−0.214	−0.214	−0.214	−0.214	−0.214	−0.214	−0.214	−0.214
12	−0.213	−0.213	−0.213	−0.214	−0.213	−0.213	−0.214	−0.214	−0.214	−0.214	−0.214	−0.214	−0.214	−0.214	−0.214
13	−0.215	−0.216	−0.216	−0.214	−0.214	−0.214	−0.214	−0.214	−0.214	−0.214	−0.214	−0.214	−0.214	−0.214	−0.214
14	−0.212	−0.210	−0.210	−0.213	−0.213	−0.213	−0.213	−0.213	−0.213	−0.214	−0.214	−0.214	−0.214	−0.214	−0.214
15	−0.217	−0.207	−0.208	−0.215	−0.216	−0.216	−0.214	−0.214	−0.214	−0.214	−0.214	−0.214	−0.214	−0.214	−0.214
16	−0.212	−0.221	−0.221	−0.212	−0.210	−0.210	−0.213	−0.213	−0.213	−0.213	−0.213	−0.213	−0.214	−0.214	−0.214
17	−0.240	−0.247	−0.247	−0.218	−0.207	−0.207	−0.215	−0.216	−0.216	−0.214	−0.214	−0.214	−0.214	−0.214	−0.214
18	−0.387	−0.382	−0.383	−0.212	−0.221	−0.221	−0.212	−0.210	−0.210	−0.213	−0.213	−0.213	−0.213	−0.213	−0.213
19				−0.240	−0.247	−0.247	−0.218	−0.207	−0.208	−0.215	−0.216	−0.216	−0.215	−0.214	−0.214
20				−0.387	−0.382	−0.382	−0.212	−0.221	−0.221	−0.212	−0.210	−0.210	−0.213	−0.213	−0.213
21							−0.240	−0.247	−0.247	−0.218	−0.207	−0.208	−0.215	−0.216	−0.216
22							−0.387	−0.382	−0.382	−0.212	−0.221	−0.221	−0.212	−0.210	−0.210
23										−0.240	−0.247	−0.247	−0.218	−0.207	−0.208
24										−0.387	−0.382	−0.382	−0.212	−0.221	−0.221
25													−0.240	−0.247	−0.247
26													−0.387	−0.382	−0.382
AVG	−0.236	−0.236	−0.236	−0.234	−0.234	−0.234	−0.232	−0.232	−0.232	−0.230	−0.230	−0.231	−0.229	−0.229	−0.229
SUM	−4.246	−4.246	−4.249	−4.675	−4.674	−4.675	−5.103	−5.103	−5.105	−5.531	−5.531	−5.533	−5.959	−5.958	−5.961

B

Atom	C50-β-carotene	Spiroloxanthin	C44-β-carotene	Lycopene	(C40-)β-carotene			Spheroidene	Lutein	C36-β-carotene	Neurosporene
					s-trans	*s-cis1*	*s-cis2*				
1	0.012	–0.196	0.012	0.017	0.028	0.029	0.012	–0.197	–0.192	0.011	0.018
2	–0.072	–0.222	–0.072	–0.248	–0.072	–0.073	–0.070	–0.222	–0.230	–0.072	–0.249
3	–0.215	–0.018	–0.215	–0.219	–0.209	–0.208	–0.212	–0.019	–0.019	–0.215	–0.217
4	–0.220	–0.219	–0.220	–0.216	–0.226	–0.226	–0.225	–0.218	–0.216	–0.220	–0.217
5	–0.020	–0.225	–0.020	–0.023	–0.016	–0.016	–0.019	–0.226	–0.226	–0.020	–0.020
6	–0.217	–0.209	–0.217	–0.216	–0.220	–0.220	–0.218	–0.208	–0.206	–0.217	–0.222
7	–0.227	–0.025	–0.227	–0.227	–0.226	–0.225	–0.226	–0.026	–0.023	–0.227	–0.211
8	–0.207	–0.213	–0.207	–0.208	–0.210	–0.210	–0.208	–0.212	–0.216	–0.208	–0.215
9	–0.026	–0.228	–0.026	–0.024	–0.024	–0.022	–0.023	–0.229	–0.212	–0.020	–0.216
10	–0.211	–0.207	–0.211	–0.217	–0.218	–0.219	–0.217	–0.205	–0.211	–0.217	–0.026
11	–0.228	–0.024	–0.224	–0.213	–0.213	–0.212	–0.213	–0.026	–0.217	–0.217	–0.207
12	–0.206	–0.216	–0.208	–0.213	–0.213	–0.214	–0.213	–0.215	–0.023	–0.020	–0.228
13	–0.024	–0.213	–0.024	–0.217	–0.218	–0.216	–0.217	–0.216	–0.207	–0.208	–0.215
14	–0.216	–0.213	–0.024	–0.024	–0.024	–0.025	–0.023	–0.210	–0.226	–0.227	–0.024
15	–0.212	–0.216	–0.208	–0.208	–0.210	–0.207	–0.208	–0.222	–0.216	–0.217	–0.215
16	–0.212	–0.024	–0.224	–0.227	–0.226	–0.227	–0.226	–0.019	–0.020	–0.020	–0.220
17	–0.216	–0.207	–0.211	–0.216	–0.220	–0.217	–0.217	–0.217	–0.218	–0.220	–0.248
18	–0.024	–0.227	–0.026	–0.023	–0.016	–0.021	–0.020	–0.217	–0.217	–0.215	0.016
19	–0.206	–0.213	–0.207	–0.216	–0.226	–0.220	–0.221	–0.249	–0.069	–0.072	
20	–0.228	–0.024	–0.227	–0.219	–0.209	–0.216	–0.214	0.018	0.010	0.011	
21	–0.211	–0.210	–0.218	–0.248	–0.072	–0.072	–0.072				
22	–0.026	–0.224	–0.020	0.017	0.028	0.012	0.012				
23	–0.207	–0.222	–0.224								
24	–0.227	–0.015	–0.212								
25	–0.217	–0.238	–0.070								
26	–0.020	–0.190	0.012								
27	–0.220										
28	–0.215										
29	–0.072										
30	0.012										
AVG	–0.153	–0.171	–0.143	–0.163	–0.146	–0.147	–0.147	–0.167	–0.158	–0.140	–0.162
SUM	–4.578	–4.437	–3.717	–3.587	–3.211	–3.224	–3.237	–3.336	–3.154	–2.809	–2.915

Table 3. CCC angles in the polyene chain for the calculated optimized geometries. Central bonds are coloured with a grey background. The *s-trans* and *s-cis* represent the positions of the ending groups. A: values for different length polyene molecules. B: values for carotenoids.

A

CCC angle	$N = 9$			$N = 10$			$N = 11$			$N = 12$			$N = 13$		
	s-trans	*s-cis1*	*s-cis2*	*s-trans*	*s-cis1*	*s-cis2*	*s-trans*	*s-cis1*	*s-cis2*	*s-trans*	*s-cis1*	*s-cis2*	*s-trans*	*s-cis1*	*s-cis2*
1–2–3	124.61	124.62	127.53	124.61	124.62	127.74	124.61	124.61	127.56	124.62	124.61	127.57	124.62	124.63	127.57
2–3–4	124.18	124.19	126.92	124.18	124.19	127.13	124.18	124.18	126.95	124.18	124.18	126.96	124.18	124.19	126.96
3–4–5	124.57	124.58	124.10	124.57	124.58	124.03	124.57	124.58	124.09	124.58	124.58	124.08	124.58	124.59	124.08
4–5–6	124.35	124.36	124.34	124.35	124.36	124.38	124.35	124.34	124.34	124.35	124.34	124.34	124.34	124.36	124.34
5–6–7	124.49	124.51	124.51	124.50	124.51	124.48	124.50	124.51	124.51	124.51	124.51	124.51	124.51	124.52	124.51
6–7–8	124.41	124.42	124.43	124.41	124.42	124.45	124.41	124.40	124.43	124.41	124.40	124.42	124.40	124.41	124.42
7–8–9	124.47	124.49	124.49	124.48	124.50	124.48	124.48	124.49	124.50	124.49	124.49	124.50	124.49	124.51	124.50
8–9–10	124.45	124.44	124.46	124.44	124.44	124.46	124.44	124.43	124.45	124.43	124.43	124.45	124.43	124.44	124.44
9–10–11	124.45	124.47	124.46	124.46	124.49	124.47	124.47	124.48	124.49	124.48	124.49	124.49	124.48	124.50	124.50
10–11–12	124.47	124.46	124.49	124.46	124.46	124.47	124.45	124.44	124.47	124.45	124.44	124.46	124.45	124.45	124.46
11–12–13	124.41	124.46	124.43	124.44	124.47	124.46	124.46	124.47	124.47	124.46	124.48	124.48	124.47	124.49	124.49
12–13–14	124.49	124.47	124.51	124.48	124.47	124.48	124.47	124.45	124.49	124.46	124.45	124.48	124.46	124.46	124.47
13–14–15	124.35	124.38	124.34	124.41	124.45	124.45	124.44	124.46	124.45	124.45	124.47	124.46	124.46	124.49	124.47
14–15–16	124.57	124.02	124.10	124.50	124.47	124.48	124.48	124.46	124.50	124.48	124.46	124.49	124.47	124.47	124.49
15–16–17	124.18	127.13	126.92	124.35	124.38	124.38	124.41	124.44	124.43	124.43	124.46	124.45	124.45	124.48	124.46
16–17–18	124.61	127.73	127.53	124.57	124.02	124.03	124.50	124.47	124.51	124.49	124.46	124.50	124.48	124.47	124.50
17–18–19				124.18	127.13	127.13	124.35	124.37	124.34	124.41	124.44	124.42	124.43	124.47	124.44
18–19–20				124.61	127.73	127.74	124.57	124.02	124.09	124.51	124.47	124.51	124.49	124.48	124.50
19–20–21							124.18	127.11	126.95	124.35	124.37	124.34	124.40	124.45	124.42
20–21–22							124.61	127.72	127.56	124.58	124.02	124.08	124.51	124.48	124.51
21–22–23										124.18	127.11	126.96	124.34	124.38	124.34
22–23–24										124.62	127.72	127.57	124.58	124.03	124.08
23–24–25													124.18	127.13	126.96
24–25–26													124.62	127.73	127.57
AVG	124.44	124.80	125.10	124.44	124.76	125.07	124.45	124.72	124.98	124.45	124.70	124.93	124.45	124.69	124.90
SUM	1991.1	1996.7	2001.6	2240	2245.7	2251.2	2488.9	2494.4	2499.6	2737.9	2743.4	2748.5	2986.8	2992.6	2997.5

B

CCC angle	C50-β-carotene	Spiroloxanthin	C44-β-carotene	Lycopene	(C40-)β-carotene			Sphe-roidene	Lutein	C36-β-carotene	Neurosporene
					s-trans	*s-cis1*	*s-cis2*				
1–2–3	122.61	126.65	122.60	127.89	117.62	117.57	123.08	126.66	126.80	122.53	127.92
2–3–4	126.09	118.32	126.13	123.18	130.79	130.85	126.55	118.32	118.25	125.86	123.16
3–4–5	126.32	128.12	126.29	126.64	125.26	125.21	126.47	128.12	128.18	126.45	126.66
4–5–6	118.19	123.08	118.27	118.40	118.17	118.22	118.14	123.11	122.94	118.19	118.40
5–6–7	128.19	126.63	128.09	128.13	128.25	128.16	128.28	126.62	126.66	128.17	128.14
6–7–8	123.04	118.34	123.15	123.11	123.10	123.21	122.92	118.38	118.27	123.04	123.67
7–8–9	126.66	128.17	126.58	126.61	126.63	126.53	126.73	128.12	128.17	126.70	123.64
8–9–10	118.32	123.04	118.39	118.35	118.37	118.42	118.28	123.12	123.55	118.19	128.16
9–10–11	128.15	126.65	128.06	128.16	128.18	128.08	128.23	126.59	123.70	127.44	118.36
10–11–12	123.06	118.30	122.77	123.63	123.67	123.79	123.56	118.36	128.07	127.44	126.64
11–12–13	126.61	128.19	126.34	123.63	123.67	123.52	123.72	128.15	118.34	118.19	123.09
12–13–14	118.31	123.57	121.99	128.16	128.18	128.26	128.11	123.64	126.56	126.70	128.16
13–14–15	128.14	123.70	121.95	118.35	118.37	118.28	118.36	123.64	123.07	123.04	118.40
14–15–16	123.61	128.10	126.42	126.61	126.63	126.73	126.60	128.15	128.10	128.17	126.72
15–16–17	123.61	118.37	122.66	123.11	123.10	122.93	123.08	118.38	118.21	118.19	123.12
16–17–18	128.14	126.56	128.15	128.13	128.25	128.27	128.15	126.63	126.27	126.45	127.94
17–18–19	118.31	123.15	118.33	118.40	118.18	118.16	118.22	123.20	126.00	125.86	
18–19–20	126.61	128.10	126.68	126.64	125.26	126.43	126.31	127.80	122.69	122.53	
19–20–21	123.05	118.39	123.04	123.18	130.79	125.90	126.01				
20–21–22	128.15	126.58	128.19	127.89	117.62	122.51	122.52				
21–22–23	118.32	123.18	118.21								
22–23–24	126.66	128.06	126.39								
23–24–25	123.04	118.43	126.70								
24–25–26	128.19	126.47	123.14								
25–26–27	118.19										
26–27–28	126.32										
27–28–29	126.09										
28–29–30	122.61										
AVG	124.09	124.09	124.11	124.41	124.00	124.05	124.17	124.28	124.10	124.06	124.51
SUM	3474.6	2978.2	2978.5	2488.2	2480.1	2481.0	2483.3	2237.0	2233.8	2233.1	1992.2

References

[1] A.A. Pascal, Z.F. Liu, K. Broess, B. van Oort, H. van Amerongen, C. Wang, P. Horton, B. Robert, W.R. Chang, and A. Ruban, Molecular basis of photoprotection and control of photosynthetic light-harvesting, Nature **436**, 134–137 (2005).

[2] A.V. Ruban, R. Berera, C. Ilioaia, I.H.M. van Stokkum, J.T.M. Kennis, A.A. Pascal, H. van Amerongen, B. Robert, P. Horton, and R. van Grondelle, Identification of a mechanism of photoprotective energy dissipation in higher plants, Nature **450**, 575–578 (2007).

[3] *Carotenoids. Volume 4: Natural Functions*, eds. G. Britton, S. Liaasen-Jensen, and H. Pfander (Birkäuser Verlag, Basel, Boston, 2008).

[4] N.E. Holt, D. Zigmantas, L. Valkunas, X.P. Li, K.K. Niyogi, and G.R. Fleming, Carotenoid cation formation and the regulation of photosynthetic light harvesting, Science **307**, 433–436 (2005).

[5] C. Curutchet and B. Mennucci, Quantum chemical studies of light harvesting, Chem. Rev. **117**, 294–343 (2017).

[6] T. Polivka and V. Sundstrom, Ultrafast dynamics of carotenoid excited states – from solution to natural and artificial systems, Chem. Rev. **104**, 2021–2071 (2004).

[7] C.S. Foote, in: *Free Radicals in Biology*, Vol. 2, ed. W.A. Pryor (Academic Press, New York, 1976) pp. 85–133.

[8] N.I. Krinsky, The evidence for the role of carotenes in preventive health, Clin. Nutr. **7**, 107–114 (1988).

[9] P. Lachance, Dietary intake of carotenes and carotene gap, Clin. Nutr. **7**, 118–122 (1988).

[10] D.L. Monego, M.B. da Rosa, and P.C. do Nascimento, Applications of computational chemistry to the study of the antiradical activity of carotenoids: A review, Food Chem. **217**, 37–44 (2017).

[11] T. Ruiz-Anchondo, N. Flores-Holguín, and D. Glossman-Mitnik, Natural carotenoids as nanomaterial precursors for molecular photovoltaics: a computational DFT study, Molecules **15**, 4490–4510 (2010).

[12] A.L. LeRosen and E.D. Reid, An investigation of certain solvent effect in absorption spectra, J. Chem. Phys. **20**, 233–236 (1952).

[13] K. Hirayama, Absorption spectra and chemical structures. I. Conjugated polyenes and *p*-polyphenyls, J. Am. Chem. Soc. **77**, 373–379 (1955).

[14] P.O. Andersson, T. Gillbro, L. Ferguson, and R.J. Cogdell, Absorption spectral shifts of carotenoids related to medium polarizability, Photochem. Photobiol. **54**, 353–360 (1991).

[15] M. Kuki, H. Nagae, R.J. Cogdell, K. Shimada, and Y. Koyama, Solvent effect on spheroidene in nonpolar and polar solutions and the environment of spheroidene in the light-harvesting complexes of *Rhodobacter sphaeroides* 2.4.1 as revealed by the energy of the $^1A_g^- \rightarrow {}^1B_u^+$ absorption and the frequencies of the vibronically coupled C=C stretching Raman lines in the $^1A_g^-$ and $^1B_u^-$ states, Photochem. Photobiol. **59**, 116–124 (1994).

[16] Z.G. Chen, C. Lee, T. Lenzer, and K. Oum, Solvent effects on the $S_0(1^1A_g^-) \rightarrow S_2(1^1B_u^+)$ transition of β-carotene, echinenone, canthaxanthin, and astaxanthin in supercritical CO_2 and CF_3H, J. Phys. Chem. A **110**, 11291–11297 (2006).

[17] I. Renge and E. Sild, Absorption shifts in carotenoids – influence of index of refraction and submolecular electric fields, J. Photochem. Photobiol. A **218**, 156–161 (2011).

[18] P. Tavan and K. Schulten, The low-lying electronic excitations in long polyenes: A PPP-MRD-CI study, J. Chem. Phys. **85**, 6602–6609 (1986).

[19] T. Polivka and V. Sundstrom, Dark excited states of carotenoids: consensus and controversy, Chem. Phys. Lett. **477**, 1–11 (2009).

[20] E. Papagiannakis, J.T.M. Kennis, I.H.M. van Stokkum, R.J. Cogdell, and R. van Grondelle, An alternative carotenoid-to-bacteriochlorophyll energy transfer pathway in photosynthetic light harvesting, Proc. Natl. Acad. Sci. USA **99**, 6017–6022 (2002).

[21] P. Wang, R. Nakamura, Y. Kanematsu, Y. Koyama, H. Nagae, T. Nishio, H. Hashimoto, and J.P. Zhang, Low-lying singlet states of carotenoids having 8–13 conjugated double bonds as determined by electronic absorption spectroscopy, Chem. Phys. Lett. **410**, 108–114 (2005).

[22] M. Macernis, J. Sulskus, C.D. Duffy, P.A.V. Ruban, and L. Valkunas, Electronic spectra of structurally deformed lutein, J. Phys. Chem. A **116**, 9843–9853 (2012).

[23] C.D.P. Duffy, J. Chmeliov, M. Macernis, J. Sulskus, L. Valkunas, and A.V. Ruban, Modeling of fluorescence quenching by lutein in the plant light-harvesting complex LHCII, J. Phys. Chem. B **117**, 10974–10986 (2013).

[24] J. Dale, Empirical relationships of the minor bands in the absorption spectra of polyenes, Acta Chem. Scand. **8**, 1235–1256 (1954).

[25] R. Hemley and B. Kohler, Electronic structure of polyenes related to the visual chromophore. A simple model for the observed band shapes, Biophys. J. **20**, 377–382 (1977).

[26] R.L. Christensen, E.A. Barney, R.D. Broene, M.G.I. Galinato, and H.A. Frank, Linear polyenes: models for the spectroscopy and photophysics of carotenoids, Arch. Biochem. Biophys. **430**, 30–36 (2004).

[27] G. Araki and T. Murai, Molecular structure and absorption spectra of carotenoids, Prog. Theor. Phys. **8**, 639–654 (1952).

[28] H. Suzuki and S. Mizuhuashi, π-electronic structure and absorption spectra of carotenoids, J. Phys. Soc. Jpn. **19**, 724–738 (1964).

[29] M. Macernis, J. Sulskus, S. Malickaja, B. Robert, and L. Valkunas, Resonance Raman spectra and electronic transitions in carotenoids: a density functional theory study, J. Phys. Chem. A **118**, 1817–1825 (2014).

[30] J.C. Dobrowolski, in: *Carotenoids: Nutrition, Analysis and Technology*, 1st ed., eds. A. Kaczor and M. Barańska (Wiley, Chichester, 2016) pp. 77–102.

[31] M. Macernis, D. Galzerano, J. Sulskus, E. Kish, Y.-H. Kim, S. Koo, L. Valkunas, and B. Robert, Resonance Raman spectra of carotenoid molecules: influence of methyl substitutions, J. Phys. Chem. A **119**, 56–66 (2015).

[32] M.M. Mendes-Pinto, E. Sansiaume, H. Hashimoto, A.A. Pascal, A. Gall, and B. Robert, Electronic absorption and ground state structure of carotenoid molecules, J. Phys. Chem. B **117**, 10974–10986 (2013).

[33] B. Robert, in: *The Electronic Structure, Stereochemistry and Resonance Raman Spectroscopy of Carotenoids*, eds. H. Frank, A. Young, G. Britton, and R. Cogdell (Kluwer Academic Publishers, Dordrecht, 1999) p. 189.

[34] Y. Koyama and R. Fujii, in: *The Photochemistry of Carotenoids*, eds. H. Frank, A. Young, G. Britton, and R. Cogdell (Kluwer Academic Publishers, Dordrecht, 1999) p. 161.

[35] M.M. Mendes-Pinto, E. Sansiaume, H. Hashimoto, A.A. Pascal, A. Gall, and B. Robert, Electronic absorption and ground state structure of carotenoid molecules, J. Phys. Chem. B **117**, 11015–11021 (2013).

[36] S. Saito and M. Tasumi, Normal-coordinate analysis of retinal isomers and assignments of Raman and infrared bands, J. Raman Spectrosc. **14**, 236–245 (1983).

[37] A. Angerhofer, F. Bornhauser, A. Gall, and R.J. Cogdell, Optical and optically detected magnetic-resonance investigation on purple photosynthetic bacterial antenna complexes, Chem. Phys. **194**, 259–274 (1995).

[38] M.J. Llansola-Portoles, R. Sobotka, E. Kish, M.K. Shukla, A.A. Pascal, T. Polívka, and B. Robert, Twisting a β-carotene, an adaptive trick from nature for dissipating energy during photoprotection, J. Biol. Chem. **292**, 1396–1403 (2017).

[39] K. Jomova and M. Valko, Health protective effects of carotenoids and their interactions with other biological antioxidants, Eur. J. Med. Chem. **70**, 102–110 (2013).

[40] T. Toury, J. Zyss, V. Chernyak, and S. Mukamel, Collective electronic oscillators for second-order polarizabilities of push–pull carotenoids, J. Phys. Chem. A **105**, 5692–5703 (2001).

[41] H. Hashimoto, T. Nakashima, K. Hattori, T. Yamada, T. Mizoguchi, Y. Koyama, and T. Kobayashi, Structures and non-linear optical properties of polar carotenoid analogues, Pure Appl. Chem. **71**, 2225–2236 (1999).

[42] V.M. Geskin, M.Yu. Balakina, J. Li, S.R. Marder, and J.L. Brédas, Theoretical investigation of the origin of the large non-linear optical response in acceptor-substituted carotenoids, Syn. Met. **116**, 263–267 (2001).

[43] S. Krawczyk, B. Jazurek, R. Luchowski, and D. Wiacek, Electroabsorption spectra of carotenoid isomers: Conformational modulation of polarizability vs. induced dipole moments, Chem. Phys. **326**, 465–470 (2006).

[44] M.Y. Balakina, J. Li, V.M. Geskin, S.R. Marder, and J.L. Bredas, Nonlinear optical response in acceptor-substituted carotenoids: A theoretical study, J. Chem. Phys. **113**, 9598–9609 (2000).

[45] W.L. Liu, D.M. Wang, Z.R. Zheng, A.H. Li, and W.H. Su, Solvent effects on the $S_0 \rightarrow S_2$ absorption spectra of β-carotene, Chinese Phys. B **19**, 013102 (2010).

[46] Z.F. Liu, H.C. Yan, K.B. Wang, T.Y. Kuang, J.P. Zhang, L.L. Gui, X.M. An, and W.R. Chang, Crystal structure of spinach major light-harvesting complex at 2.72 angstrom resolution, Nature **428**, 287–292 (2004).

[47] M.J. Frisch, G.W. Trucks, H.B. Schlegel, G.E. Scuseria, M.A. Robb, J.R. Cheeseman, G. Scalmani, V. Barone, B. Mennucci, G.A. Petersson, et al. *Gaussian 09* (Gaussian, Inc., Wallingford, CT, USA, 2009).

[48] J. Heyd, G.E. Scuseria, and M. Ernzerhof, Hybrid functionals based on a screened Coulomb potential, J. Chem. Phys. **118**, 8207 (2003).

[49] C.D.P. Duffy, M.P. Johnson, M. Macernis, L. Valkunas, W. Barford, and A.V. Ruban, A theoretical investigation of the photophysical consequences of major plant light-harvesting complex aggregation within the photosynthetic membrane, J. Phys. Chem. B **114**, 15244–15253 (2010).

[50] T. Yanai, D.P. Tew, and N.C. Handy, A new hybrid exchange–correlation functional using the Coulomb-attenuating method (CAM-B3LYP), Chem. Phys. Lett. **393**, 51–57 (2004).

[51] A. Dreuw, P.H.P. Harbach, J.M. Mewes, and M. Wormit, Quantum chemical excited state calculations on pigment–protein complexes require thorough geometry re-optimization of experimental crystal structures, Theor. Chem. Acc. **125**, 419–426 (2010).

[52] T. Kupka, A. Buczek, M.A. Broda, M. Stachów, and P. Tarnowski, DFT studies on the structural and vibrational properties of polyenes, J. Mol. Model. **22**, 101 (2016).

[53] S.R. Pilli, T. Banerjee, and K. Mohanty, HOMO–LUMO energy interactions between endocrine disrupting chemicals and ionic liquids using the density functional theory: Evaluation and comparison, J. Mol. Liq. **207**, 112–124 (2015).

RAMANO ν_1 JUOSTOS IR GLOBALIŲ SKALIARINIŲ SAVYBIŲ NETIESINĖS KORELIACIJOS ĮVAIRAUS ILGIO KAROTINOIDUOSE

M. Mačernis

Vilniaus universiteto Cheminės fizikos institutas, Vilnius, Lietuva

Santrauka

Skirtingo ilgio karotinoidų ir polienų molekulių poliarizacinės savybės, kurios sietinos su Ramano ν_1 juosta, buvo teoriškai analizuotos naudojant tankio funkcionalų metodiką. Karotinoidų ir polienų monomerų poliarizacija ir kitos savybės buvo skaičiuojamos naudojant globalias skaliarines savybes. Rezultatai rodo tiesinę priklausomybę tarp Ramano ν_1 juostos atitinkamo virpesinio dažnio, kuris atitinka C = C jungties pailgėjimo modą, ir globalaus kietumo (ir globalaus minkštumo) visoms skirtingo ilgio molekulėms. Visos tiesinės priklausomybės tarp jungties ilgio ir visų globalių skaliarinių savybių buvo tik polieninėms struktūroms. Remiantis skaičiavimų rezultatais buvo nustatytas papildomas sąryšis: dėl *s-cis*-izomerizacijos padidėjo polienų efektyvusis jungties ilgis ir globalus minkštumas, o karotinoidų, kurie turi galuose β-žiedus, efektyvus jungties ilgis ir globalus minkštumas sumažėjo. Pagal elektrofiliškumo indeksų analizę krūvio pernašos (CT) vyksmai turėtų lengviau vykti ilgesniuose karotinoidų ir polienų dariniuose. Elektroneigiamumo tiesinės priklausomybės buvo tarp polienų ir tarp atskirų karotinoidų pogrupių molekulių. Prie karotinoidų polieninės grandinėlės prijungtos įvairios grupės ypač turėjo reikšmės elektrofiliškumo indeksui. Karotinoidų efektyvus jungties ilgis nėra tiesiškai susijęs su elektroneigiamumu, cheminiu potencialu ir elektrofiliškumo indeksu, tačiau beveik tiesinė priklausomybė matoma su globaliu kietumu, tuo tarpu polieninių darinių modeliai tiesines priklausomybes turėjo visada.